Asian Research Journal of Mathematics

10(1): 1-20, 2018; Article no.ARJOM.42092
ISSN: 2456-477X

Squeezing Nanofluid Flow between Two Parallel Plates under the Influence of MHD and Thermal Radiation

Sher Muhammad[1,2*], Syed Inayat Ali Shah[1], Gohar Ali[1], Mohammad Ishaq[1], Syed Asif Hussain[1,2] and Hidayat Ullah[2]

[1]Department of Mathematics, Islamia College Peshawar, 25000, KP, Pakistan.
[2]CECOS University of IT and Emerging Sciences, Peshawar, 25000, KP, Pakistan.

Authors' contributions

This work was carried out in equal collaboration of all the authors. The final version of the manuscript has been read and approved by the authors.

Article Information

DOI: 10.9734/ARJOM/2018/42092
Editor(s):
(1) Nikolaos Dimitriou Bagis, Department of Informatics and Mathematics, Aristotelian University of Thessaloniki, Greece.
Reviewers:
(1) Mohamed A. Hassan, Ain Shams University, Egypt.
(2) Animasaun Isaac Lare, Federal University of Technology, Nigeria.
Complete Peer review History: http://www.sciencedomain.org/review-history/25139

Original Research Article

Received: 28th March 2018
Accepted: 7th June 2018
Published: 14th June 2018

Abstract

This article addresses the squeezing nanofluid flow between two parallel plates under the influence of magneto hydrodynamics (MHD) and thermal radiation. One of the plates is fixed and the other is kept stretched. In this study water is considered as a base fluid. Heat and mass transfer aspects are examined in the presence of thermophoresis and Brownian motion. Appropriate variables lead to a strong nonlinear ordinary differential system. The acquired nonlinear system has been solved via the homotopy analysis method (HAM). The convergence of the method has been shown numerically. Also, we obtained Skin friction, local Nusselt number and Sherwood number discussed with reference to flow parameters. The variation of the Skin friction, Nusselt number, Sherwood number and their impacts on the velocity, concentration and temperature profiles are examined.The effects of non-dimensional parameters on velocity, temperature and concentration have been discussed with the help of graphs for both suction and injection cases .Moreover, for comprehension the physical presentation of the embedded parameters, such as unsteady squeezing parameter, Thermal radiation parameter, Peclet number, Thermophoresis parameter, Levis number, Prandtl number, Schmidt number and Brownian motion are plotted and discussed graphically. At the end, we make some concluding remarks in the light of this article.

Keywords: Thermal radiation; nanofluid; MHD; parallel plates; squeezing flow and HAM.

**Corresponding author: E-mail: shermuhammad@cecos.edu.pk;*

1 Introduction

Squeezing nanofluid flow between two parallel plates under the Influence of MHD and Thermal Radiation plays a very important role in the real world phenomena which attract the researcher due to its vast applications. Many scientists worked in this field, according to their levels and needs. Squeezing flow has several applications in different fields, particularly in chemical engineering and food industry. Some publications are available to explain and demonstrate the properties and behaviour of squeezing nanofluid for industrial applications like nuclear reactions, foods, electronics, biomechanics, transportations etc. There are several examples regarding squeezing flow, but especially the important ones are injected, compression and polymer preparation. This field got considerable attention due to useful applications in the Biophysical and Physical field. Verma [1] has been studied squeezing flow amongst parallel plates. The unsteady squeezing flow of a viscous fluid between parallel disks has many applications in hydro dynamical machines, transient loading of mechanical components, and the squeezed films in power transmission. The flow configuration also has relevance in bearings with liquid metal lubrication. Magneto hydrodynamic (MHD) fluid can be treated as a lubricant to prevent the unexpected variation of lubricant viscosity with temperature under certain extreme operating conditions. The seminal work on squeezing flow under lubrication approximation was reported by Stefan [2]. Singh et al. [3] has been highlighted mass relocation and the effect of thermophoresis and Brownian motion. Hayat et al. [4] has been explored magneto-hydrodynamic (MHD) in squeezing flow in Jeffery nanofluid for the parallel disc. Dib et al. [5] has been investigated squeezing nanofluid flow analytically. The term nanofluid was envisioned to describe a fluid in which nanometer-sized particles were suspended in conventional heat transfer basic fluids. Nanotechnology aims to manipulate the structure of the matter at the molecular level with the goal for innovation in virtually every industry and public endeavor, including biological sciences, physical sciences, electronics cooling, transportation, the environment and national security. Nano-fluid is the composition of Nano-particles, which shows significant properties at a reticent concentration of Nano-particles. Nano-fluid is a term refers to liquid consisting sub microparticles. It has abundant applications, but the important feature is the development of thermal conductivity observed by Masuda et al. [6]. His investigation reveals that Nano-fluid has different thermal properties like thermal viscosity, thermal infeasibility, relocate of temperature, convection temperature and thermal conductivity as compared to oil and water base fluids [7-9]. Magneto hydrodynamics (MHD; also magneto-fluid dynamics or hydro magnetic) is the study of the magnetic properties of electrically conducting fluids. Examples of such magneto fluids include plasmas, liquid metals, salt water, and electrolytes. Muhammad et al. [10] investigated the rotating flow of magneto hydrodynamic carbon nanotubes over a stretching sheet with the impact of non-linear thermal radiation and heat generation/absorption. Hamad [11] has been investigated the Nano-fluid analytical solution for convection flow in the occurrence of a magnetic field. Thermal radiation, a process by which energy, in the form of electromagnetic radiation, is emitted by a heated surface in all directions and travels directly to its point of absorption at the speed of light; thermal radiation does not require an intervening medium to carry it. Khan et al. [12] studied the combined magneto hydrodynamic and electric field effect on an unsteady Maxwell nanofluid flow over a stretching surface under the influence of variable heat and thermal radiation. Sheikholeslami [13] has been investigated thermal radiation effect on MHD flow and relocate of temperature by two-phase mode. The flow of nano-fluid among parallel plates is one of the benchmark problems which have important and crucial applications in MHD, the examples are power generators, pumps, purification of crude oil, petroleum industry, aerodynamic heating, different automobiles sprays and designing cooling systems with liquid metal. Goodman [14] was the first one to investigate viscous fluid in parallel plates. Borkakoti and Bharali [15] have been investigated Hydro magnetic viscous flow among parallel plates where one of the plates is a stretching sheet. Attia et al. [16] has been examined viscous flow between parallel plates with magnetohydrodynamics. Sheikholeslami et al. [17-19] has been studied the nanofluid flow of viscous fluids between parallel plates with rotating systems in three dimensions under the magneto hydrodynamics (MHD) effects. For the solution of the modelled problems they used numerical techniques and described the special effects of achieving parameters in detail. Mahmoodi and Kandelousi [20] have examined the hydro magnetic impact of Kerosene−alumina nanofluid flow in the occurrence of heat transfer analysis, differential transformation method is used in their work. Tauseef et al. [21] and Rokni et al. [22] have been scrutinized the MHD and temperature effects on nanofluids flow in parallel plates with the rotating system. Azimi and Riazi [23] have been studied temperature transfer analysis of CO-Water Nano-

fluid flow between two parallel disks. Thermal radiation has an important role in flow phenomena. It has various applications because of its dependence on the temperature difference, as the polymer processing industries are using the radiation effects for the transformation of heat. The common ways of transfer of heat in the industry is not beneficial nowadays. The radiations play a significant role in heat transfer. Hayat et al. [24] has been discussed thermal radiations influence in squeezing flows of Jeffery fluids. Ali et al. [25] have been discussed the effect of radiations on un-steady free convection magnetohydrodynamics flows of the Brinkman kind fluids in a porous medium have Newtonian heat. Khan et al. [26] have been observed thermal radiation effect on squeezing flow Casson fluid among parallel disks. Makinde et al. [27] investigated thermophoresis and brownian motion effects on MHD bioconvection of nanofluid with nonlinear thermal radiation and quartic chemical reaction past an upper horizontal surface of a paraboloid of revolution. Avinash et al. [28] investigated aligned magnetic field effect on radiative bioconvection flow past a vertical plate with thermophoresis and brownian motion. Mahanthesh et al. [29] investigated Exploration of Non-Linear Thermal Radiation and Suspended Nanoparticles Effects on Mixed Convection Boundary Layer Flow of Nano liquids on a Melting Vertical Surface. Pop et al. [30] studied Scrutinization of the effects of the Grashof number of the flow of different fluids driven by convection over various surfaces.

In the present field of science and engineering, most of the mathematical problems are so involved that the accurate solution is almost complicated. So for the solution of such problems, Numerical and Analytical methods are used to find the approximate solution. One of the critical and famous techniques for solving such type problems is HAM (Homotopy Analysis Method). It is a substitute method, and its main advantage is applying to the nonlinear differential equations without discretisation and linearization. In (1992) Liao [31-36] was the first one to examine this technique for the solution of non-linear problem's and showed that this technique is rapidly converging to the approximate solution. Also, this method gives us a series solution. The solution by this technique is perfect because it contains all the physical parameters of a problem and we can easily explain its performance in detail. Due to its rapid convergence, many researchers like Abbasbandy [37-38] and Rashidi [39-40] have used this technique to solve highly nonlinear and coupled equations. Hussain et al. [41] investigated Bioconvection model for squeezing flow between parallel plates containing gyrotactic microorganisms with impact of thermal radiation and heat generation/absorption by applying HAM.

The basic theme of this paper is to discuss the unsteady squeezing flow of a nanofluid between two parallel plates under the Influence of MHD and Thermal Radiation. To our knowledge, no studies have been made to analyze the simultaneous effects of heat generation/absorption on heat and mass transfer of Squeezing nanofluid between two parallel channels. The governing coupled nonlinear partial differential equations are reduced to a system of coupled ordinary differential equations using appropriate transformations, and then the resulting equations are solved analytically by the homotopy analysis method (HAM). A parametric study is conducted to investigate the influence of various physical parameters on the velocity, temperature and concentration profile. Many similar results have been found and discussed graphically. Mathematica software is used for numerical simulation.

2 Mathematical Formulation of the Problem

The calculations and modelling used in this endeavor are explained as:

The unsteady, two-dimensional and symmetric-nature flow of a viscous incompressible fluid between two parallel plates with the effects of MHD and thermal radiations is considered. The plates are placed in the Cartesian coordinates system in such a way that the lower plate is on the horizontal x-axis, and the y-axis is at the perpendicular position to the lower plate and the lower plate is fixed. It is assumed that the distance between these parallel plates is $y = h$, where h is a function of t. Furthermore, it is assumed that the lower plate is capable of moving away or towards the lower plate placed at $y = 0$. This plate (upper Plate) moves with $v(t) = \frac{dh}{dt}$ and the constant magnetic-field B_0 is acting in the y-direction. The temperatures at the upper and lower plates are T_1 and T_2, respectively. It is also assumed that both plates (upper and lower) are maintained at constant temperature. The upper plate (placed at $y = h\ (t)$) has passive auxiliary conditions and

nanoparticles are distributed constantly at the lower plate (placed at $y = 0$). Nanoparticles are diluted in the base fluid uninterruptedly and stably. The nanoparticles are scattered uniformly on the lower plate. The geometry of the nanofluid flow phenomena is shown in Fig. 1.

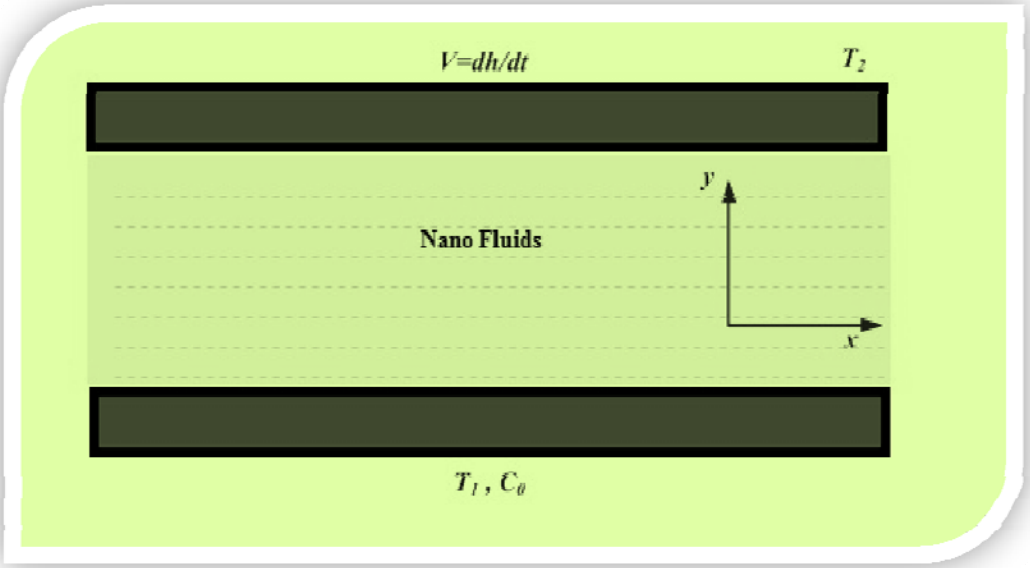

Fig. 1. Geometry of the problem

Observance in the above deliberation, the elementary equations are continuity, velocity, heat and concentration are articulated [41] as follow,

$$u_x + v_y = 0, \tag{1}$$

$$\rho\left(u_t + uu_x + vv_y\right) = -p_x + \mu\left(u_{xx} + v_{yy}\right) - \sigma B_0^2 u(t), \tag{2}$$

$$\rho_{nf}\left(v_t + uv_x + vv_y\right) = -p_y + \mu\left(v_{xx} + v_{yy}\right), \tag{3}$$

$$\left(\mathrm{T}_t + u\mathrm{T}_x + v\mathrm{T}_y\right) = \hat{\alpha}\left(\mathrm{T}_{xx} + \mathrm{T}_{yy}\right) + \tau\left[D_B\left\{C_x\mathrm{T}_x + C_y\mathrm{T}_y\right\} + \left(\frac{D_T}{\mathrm{T}_0}\right)\left\{T_x^{\,2} + T_y^{\,2}\right\}\right] - \frac{1}{\left(\rho c_p\right)_f}\frac{\partial q_{rd}}{\partial y}$$

(4)

$$C_t + uC_x + vC_y = D_B\left\{C_{xx} + C_{yy}\right\} + \frac{D_T}{\mathrm{T}_o}\left\{T_{xx} + T_{yy}\right\} \tag{5}$$

In equations (1-5) u & v denotes velocity components, T and C represents the temperature at the plate & volumetric fraction of the nanoparticles , $\tau = \dfrac{(\rho c)_p}{(\rho c)_f}$, where $(\rho c)_p$ & $(\rho c)_f$ represents temperature

capacity of nanoparticles and fluids. Moreover, ρ is the density of the nanofluid, μ denotes viscosity, D_B represents Brownian diffusion and D_T denotes thermophore tic coefficient, in x and y direction respectively. In Eq. (4), q_{rad} is the radiative heat fluctuation is expressed in term of Roseland approximation as:

$$q_{rd} = -\frac{4\sigma^*}{3\mathrm{K}^*}\frac{\partial\left(\mathrm{T}^4\right)}{\partial y}, \tag{6}$$

In Eq. (6) relation σ^*, k^* indicate the "Stefan Boltzmann" constant & "mean absorption" coefficient respectively. Supposing that the difference in heat inside the flow is such that T^4 can be expressed as a linear combination of the heat, we enlarges T^4 as Taylor's series about T_0 as under:

$$\mathrm{T}^4 = \mathrm{T}_0^4 + 4\mathrm{T}_0^3\left(\mathrm{T}-\mathrm{T}_0\right)+..., \tag{7}$$

After ignoring terms of higher order, we obtained:

$$\mathrm{T}^4 \cong -3\mathrm{T}_0^4 + 4\mathrm{T}_0^3\mathrm{T}, \tag{8}$$

By Putting Eq. (7) in Eq. (6) we get

$$\frac{\partial q_{rd}}{\partial y} = -\frac{16\mathrm{T}_0^3\sigma^*}{3K^*}\frac{\partial^2\mathrm{T}}{\partial y^2}, \tag{9}$$

For lower and upper plates feasible auxiliary conditions [42] are:

$$v = 0,\ u = 0,\ \ C = C_0, \& \ \mathrm{T} = \mathrm{T}_1\ , \tag{10}$$

$$v = \frac{dh}{dt},\ u = 0,\ \ \mathrm{T} = T_2,\ \& \ D_B\left(\frac{\partial C}{\partial y}\right) + \frac{D_T}{\mathrm{T}_0}\left(\frac{\partial \mathrm{T}}{\partial y}\right) = 0\ . \tag{11}$$

For the flow model the non-dimensional similarity variables [42] are:

$$\begin{aligned} &\Psi(x,y) = \left(\frac{1-\alpha t}{bv}\right)^{\frac{-1}{2}} xf(\eta), u = \left(\frac{1-\alpha t}{bx}\right)^{-1} f'(\eta), v = -\left(\frac{1-\alpha t}{bv}\right)^{\frac{-1}{2}} f(\eta), \eta = \left(\frac{v(1-\alpha t)}{b}\right)^{\frac{-1}{2}} y, \\ &\theta(\eta) = \left(\frac{\mathrm{T}-\mathrm{T}_0}{\mathrm{T}_2-\mathrm{T}_0}\right) \text{ and } \phi(\eta) = -1+\frac{C}{C_0}\ . \end{aligned} \tag{12}$$

In above expression T_0 and C_0 are reference temperature, reference concentration of nanoparticles and reference concentration of microorganism respectively. Moreover substituting Eq. (12) into the governing equations. (1) to (5), clearly Eq. 1 hold identically and we develop the subsequent succeeding transformed ODE's that are given bellow:

$$f^{iv} + ff''' - ff'' - \lambda\eta f''' - 3\lambda f'' - \mathrm{M}f'' = 0, \tag{13}$$

$$\left(1+\frac{4}{3}\mathrm{Rd}\right)\theta''+\mathrm{Pr}\left(f-\lambda\eta\right)\theta'+Nb\phi'\theta'+Nt\left(\theta'\right)^2=0, \tag{14}$$

$$\phi''+Le\left(f-\lambda\eta\right)\phi'+\left(\frac{\mathrm{N}t}{\mathrm{N}b}\right)\theta''=0, \tag{15}$$

In the above model equations (13) to (15) different parameters are used like λ represent unsteady squeezing parameter, thermal radiation (Rd), Brownian motion $\left(Nb\right)$, Peclet (Pe), thermophoresis parameter (Nt), Levis number $\left(\mathrm{Le}\right)$, Prandtl number (Pr) and Schmidt number $\left(Sc\right)$. Also ω, δ_ϕ and δ_θ all are constants. All these physical quantities are equal to the following expression's which are expressed as:

$$\begin{aligned}
&\lambda=\frac{\alpha}{2b},\ M=\frac{\sigma B_0^{\,2}}{\rho b}(1-\alpha t),\ Rd=\frac{4T^3\sigma}{3\left(\rho c_p\right)_f k\alpha},\mathrm{N}t=\frac{(\rho c)_p}{(\rho c)_f}\frac{D_T(\mathrm{T}_2-\mathrm{T}_0)}{\mathrm{T}_0\alpha},\\
&Nb=\frac{(\rho c)_p}{(\rho c)_f}\frac{D_bC_0}{\alpha},\ \mathrm{Pr}=\frac{\nu}{\alpha},\ Sc=\frac{\nu}{D_n},\ Pe=\frac{b_cW_c}{D_n},\ Le=\frac{\nu}{D_B},\omega=\frac{\alpha H}{2(\nu b)^{\frac{1}{2}}},\\
&\delta\phi=\left(\frac{C_1-C_0}{C_0}\right),\ \delta\theta=\frac{(\mathrm{T}_1-\mathrm{T}_0)}{(\mathrm{T}_2-\mathrm{T}_0)}.
\end{aligned} \tag{16}$$

In above mentioned equation b_c is the chemotaxis constant, W_c is the maximum cell swimming speed and D_n is the microorganism diffusion coefficient. Furthermore, transmuted form of the feasible boundary conditions, both for lower as well as for upper plates defined in equations (10) to (11) are as:

$$\begin{aligned}
&f(0)=0,\ f'(0)=0,\ f'(1)=0,\ f(1)=w,\theta(1)=\delta_\theta,\\
&\theta(0)=1,\phi(1)=\delta_\phi,\ \phi(0)\mathrm{N}b+\theta'(0)\mathrm{N}t=0.
\end{aligned} \tag{17}$$

The "Skin-Friction", "Nusselt-Number" and "Sherwood-Number" are defined under as:

$$\begin{aligned}
&C_f=\frac{2\tau\omega}{\rho U_\omega^{\,2}},\mathrm{Nu}_x=\frac{x\,\mathrm{q}_w}{\mathrm{K}\left(\mathrm{T}_w-\mathrm{T}_0\right)},Sh_x=\frac{xq_m}{D_B\left(C_w-C_0\right)},\\
&\tau_\omega=\left|\mu\frac{\partial u}{\partial y}\right|_{y=0},q_\omega=\left|\mathrm{K}\frac{\partial\mathrm{T}}{\partial y}\right|_{y=0}\ \&\ q_m=\left|-D_B\frac{\partial\phi}{\partial y}\right|_{y=0}.
\end{aligned} \tag{18}$$

In above expression T_w and C_w are surface temperature and surface concentration respectively.

By using Eq. (12) dimensionless form, Nusselt Number, Skin-Friction and Sherwood are as:

$$\frac{\sqrt{\mathrm{Re}_x}}{2} C_f = f''(0), Nu_x \,\mathrm{Re}_x^{\frac{-1}{2}} = -\theta'(0) \,\&\, Sh_x \,\mathrm{Re}_x^{\frac{-1}{2}} = -\phi'(0) \tag{19}$$

Where $\mathrm{Re}_x = \frac{xU_\omega}{\nu}$ is represents a local Reynolds number.

3 Methodology

To solve equations. (13) - (15) with boundary conditions (17), we apply "Homotopy Analysis Method (HAM) [31-36]". For the solution HAM scheme has benefits such as it is free from the large or small parameters. This technique gives a simple way to confirm the convergence of the solution. Moreover, it delivers freedom for the right selection of auxiliary parameter & base function. In this scheme, the assisting parameters $\hbar$ are used to control the convergence of the problem. The initial guesses and linear operators for the dimensionless momentum, energy and concentration equations are (f_o, θ_0, ϕ_o) and ($L_f, \mathrm{L}_\theta, L_\phi$) These are presented in the forms:

$$\begin{aligned} &f_o(\eta) = 3\omega\eta^2 - 2\omega\eta^3,\ \theta_0(\eta) = 1 - \eta + \delta_\theta\eta, \\ &\phi_o(\eta) = \frac{1}{\mathrm{N}b}(-\mathrm{N}t + \mathrm{N}t\eta + \mathrm{N}t\delta_\theta - \mathrm{N}t\delta_\theta\eta + \mathrm{N}b\delta_\phi), \end{aligned} \tag{20}$$

Selected linear operators, are:

$$L_f(\mathrm{f}) = \frac{\partial^4 f}{\partial\eta^4},\ \mathrm{L}_\theta(\theta) = \frac{\partial^2\theta}{\partial\eta^2} \text{ and } \mathrm{L}_\phi(\phi) = \frac{\partial^2\phi}{\partial\eta^2}. \tag{21}$$

The above-mentioned differential operator's contents are shown below:

$$\boldsymbol{L}_f(\varepsilon_1 + \varepsilon_2\eta + \varepsilon_3\eta^2 + \varepsilon_4\eta^3) = 0, \boldsymbol{L}_\theta(\varepsilon_5 + \varepsilon_6\eta) = 0, \boldsymbol{L}_\phi(\varepsilon_7 + \varepsilon_8\eta) = 0. \tag{22}$$

Here $\sum_{i=1}^{10} \varepsilon_i$ where $i = 1, 2, 3...$ denotes arbitrary constants.

The resultant non-linear operators are given by: N_f, N_θ, and N_ϕ

$$\begin{aligned} \mathrm{N}_\mathrm{f}\left(f(\eta;\psi)\right) = {} & \frac{\partial^4 f(\eta;\psi)}{\partial\eta^4} + f(\eta;\psi)\frac{\partial^2 f(\eta;\psi)}{\partial\eta^2} - \frac{\partial f(\eta;\psi)}{\partial\eta} \times \frac{\partial^2 f(\eta;\psi)}{\partial\eta^2} - \lambda\eta\frac{\partial^3 f(\eta;\psi)}{\partial\eta^3} \\ & -3\lambda\frac{\partial^2 f(\eta;\psi)}{\partial\eta^2} - M\frac{\partial^2 f(\eta;\psi)}{\partial\eta^2}, \end{aligned} \tag{23}$$

$$\begin{aligned} \mathrm{N}_\theta\left(\theta(\eta;\psi), f(\eta;\psi), \phi(\eta;\psi)\right) = {} & \left(1 + \frac{4}{3}Rd\right)\frac{\partial^2\theta(\eta;\psi)}{\partial\eta^2} + \mathrm{Pr}\left(f(\eta;\psi) - \lambda\eta\right)\frac{\partial\theta(\eta;\psi)}{\partial\eta} \\ & + \mathrm{N}b\frac{\partial\theta(\eta;\psi)}{\partial\eta}\frac{\partial\phi(\eta;\psi)}{\partial\eta} + \mathrm{N}t\left(\frac{\partial\theta(\eta;\psi)}{\partial\eta}\right)^2, \end{aligned} \tag{24}$$

$$\mathrm{N}_{\phi}\left(\phi(\eta;\psi),\, f(\eta;\psi),\theta(\eta;\psi)\right)=\frac{\partial^2\phi(\eta;\psi)}{\partial\eta^2}+Le\left(f(\eta;\psi)-\lambda\eta\right)\frac{\partial\phi(\eta;\psi)}{\partial\eta}$$
$$+\left(\frac{\mathrm{N}t}{\mathrm{N}b}\right)\frac{\partial^2\theta(\eta;\psi)}{\partial\eta^2}, \tag{25}$$

3.1 Zeroth-order deformation problem

Expressing $\psi\in[0,1]$ be the embedding parameter with associated parameters $\hbar_{\theta}$, $\hbar_{\phi}$ & $\hbar_{f}$ where $\hbar\neq 0$. Then the problem in case of zero order is formed as bellow:

$$(1-\psi)\boldsymbol{L}_{f}\left(f(\eta,\psi)-f_0(\eta)\right)=\psi h_{f}\mathrm{N}_{f}\left(f(\eta,\psi)\right), \tag{26}$$

$$(1-\psi)\boldsymbol{L}_{\theta}\left(\theta(\eta,\psi)-\theta_0(\eta)\right)=\psi h_{\theta}\mathrm{N}_{\theta}\left(\theta(\eta;\psi),\, f(\eta;\psi),\phi(\eta;\psi)\right), \tag{27}$$

$$(1-\psi)\boldsymbol{L}_{\phi}\left(\phi(\eta,\psi)-\phi_0(\eta)\right)=\psi h_{\phi}\mathrm{N}_{\phi}\left(\phi(\eta;\psi),\, f(\eta;\psi),\theta(\eta;\psi)\right), \tag{28}$$

The subjected boundary conditions are derived as:

$$f(\eta;\psi)\Big|_{\eta=0}=0,\ \left.\frac{\partial f(\eta;\psi)}{\partial\eta}\right|_{\eta=0}=0,\ \ f(\eta;\psi)\Big|_{\eta=1}=w,\ \left.\frac{\partial f(\eta;\psi)}{\partial\eta}\right|_{\eta=1}=0,$$
$$\theta(\eta;\psi)\Big|_{\eta=0}=1,\ \ \theta(\eta;\psi)\Big|_{\eta=1}=\delta_{\theta},\ \ \mathrm{N}b\phi(\eta;\psi)\Big|_{\eta=0}+\mathrm{N}t\left.\frac{\partial\theta(\eta;\psi)}{\partial\eta}\right|_{\eta=0}=0, \tag{29}$$
$$\phi(\eta;\psi)\Big|_{\eta=1}=\delta_{\phi},\ .$$

Where $\psi\in[0,1]$ is the imbedding constraint, $\hbar_{f}$, $\hbar_{\theta}$ and $\hbar_{\phi}$ were used to regulate convergence of the solution. Where $\psi=0$ & $\psi=1$ we have:

$$f(\eta;1)=f(\eta),\ \ \theta(\eta;1)=\theta(\eta),\ \ \phi(\eta;1)=\phi(\eta).$$

Expanding the above term of ψ with the use of Taylor's series expansion we obtain:

$$f(\eta,\psi)=f_o(\eta)+\sum_{i=1}^{\infty}f_i(\eta),\ \ \theta(\eta,\psi)=\theta_o(\eta)+\sum_{i=1}^{\infty}\theta_i(\eta),$$
$$\phi(\eta,\psi)=\phi_o(\eta)+\sum_{i=1}^{\infty}\phi_i(\eta). \tag{30}$$

Where

$$f_{\mathrm{i}}(\eta)=\frac{1}{\mathrm{i}!}\left.\frac{\partial f(\eta;\psi)}{\partial\eta}\right|_{\psi=\circ},\ \ \theta_i(\eta)=\frac{1}{\mathrm{i}!}\left.\frac{\partial\theta(\eta;\psi)}{\partial\eta}\right|_{\psi=\circ},\ \phi_i(\eta)=\frac{1}{\mathrm{i}!}\left.\frac{\partial\phi(\eta;\psi)}{\partial\eta}\right|_{\psi=\circ}. \tag{31}$$

3.2 I^{th} order deformation problem

Differentiating Zeroth Order equations i^{th} times we obtained the i^{th} Order deformation equations with respect to ψ dividing by $i!$ and then inserting $\psi = 0$. So i^{th} order deformation equations are:

$$\begin{aligned} &\boldsymbol{L}_f\left(f_i(\eta)-\xi_i f_{i-1}(\eta)\right)=h_f\Re_i^f(\eta),\boldsymbol{L}_\theta\left(\theta_{ii}(\eta)-\xi_i\theta_{i-1}(\eta)\right)=h_\theta\Re_i^\theta(\eta),\\ &\boldsymbol{L}_\phi\left(\phi_i(\eta)-\xi_i\phi_{i-1}(\eta)\right)=h_\phi\Re_i^\phi(\eta). \end{aligned} \tag{32}$$

The resultant boundary conditions are:

$$\begin{aligned} &f_i(0)=0,\ f_i'(0)=0,\ f_i(1)=0,\ f_i'(1)=0,\ \theta_{ii}(0)=0,\ \theta_{ii}(1)=0,\\ &\mathrm{N}b\phi_i(0)+\mathrm{N}t\theta_i'(0)=0,\phi_i(1)=0. \end{aligned} \tag{33}$$

$$\Re_i^f(\eta)=f_{i-1}^{iv}+\sum_{k=0}^{i-1}f_{i-1-k}f_k'''-\sum_{k=0}^{i-1}f_{i-1-k}'f_k''-\lambda\eta f_{i-1}'''-3\lambda f_{i-1}''-Mf_{i-1}'', \tag{34}$$

$$\Re_i^\theta(\eta)=\left(1+\frac{4}{3}Rd\right)\theta_{i-1}''+\mathrm{Pr}\left(\sum_{k=0}^{i-1}f_{i-1-k}\theta_k'-\lambda\eta\theta_{i-1}'\right)+\mathrm{N}b\sum_{k=0}^{i-1}\phi_{i-1-k}'\theta_k'+\mathrm{N}t\sum_{k=0}^{i-1}\theta_{i-1-k}'\theta_k', \tag{35}$$

$$\Re_i^\phi(\eta)=\phi_{i-1}''+Le\left(\sum_{k=0}^{i-1}f_{i-1-k}\phi_k'-\lambda\eta\phi_{i-1}'\right)+\left(\frac{\mathrm{N}t}{\mathrm{N}b}\right)\theta_{i-1}'', \tag{36}$$

Where

$$\xi_i=\begin{cases}1, & \text{if } \psi>1\\ 0, & \text{if } \psi\le 1\end{cases} \tag{37}$$

4 Convergence of HAM

When the series solutions are computed for the velocity, temperature and concentration functions via using HAM, the assisting parameters are $\hbar_f$, $\hbar_\varphi$ and $\hbar_\theta$. These main parameters are responsible for the convergence of the solution. The Table 1 shows the convergence of the problem. It is clear from the Table 1 that homotopy analysis technique is a quickly convergent technique.

Table 1. Displays Convergence of the HAM up to 15th Order Approximation where, $\lambda = M = Nt = 0.5$, $Sc = 0.8, \mathrm{Pr} = 0.7, Rd = 0.1, Nb = 1, Le = 0.6, \omega = 0.1$ and $Pe = 0.7$.

Approximation Order.	$f''(0)$	$\theta'(0)$	$\phi'(0)$
1	3.98886	-0.0207921	0.953750
3	3.97650	-0.0387064	0.913169
5	3.97584	-0.0396453	0.910490
7	3.97583	-0.0396677	0.910383
9	3.97583	-0.0396682	0.910379
13	3.97583	-0.0396682	0.910379
15	3.97583	-0.0396682	0.910379

5 Numerical Results and Discussion

The current research has been carried out to study the Squeezing Nanofluid Flow between Two Parallel Plates under the Influence of MHD and Thermal Radiation. The determination of this subsection is to examine the physical outcomes of dissimilar embedding on the Velocity $f(\eta)$, Heat $\theta(\eta)$ and Concentration $\phi(\eta)$ distribution which are illustrated in Figs. (2-14). Fig. 1 shows the geometry of the fluid model. The following results with complete details are achieved: Fig. 1 shows the geometry of the fluid model for comprehensions of the readers. Figs. 2, 3 and 4 represents the influences of squeezing fluid parameter λ on $f(\eta)$, $\theta(\eta)$ and $\phi(\eta)$ When plates are moving apart, then λ takes the positive value in that corresponding case & when plates are coming closer the values are considered negative. Fig. 2 shows the influence of the flow when plates are moving away & this is the opposite case of when plates are coming nearer. With the increase of λ values fluid velocity also increasing. Clearly velocity increases in the channel when fluid sucked inside. On the other hand, when fluid injected out, then the plates come closer to one another. This manner brings about a drop in the fluid and consequently decreases the velocity. With the varying value of λ parameter the influence of $f(\eta)$ shown in Fig. 2. Figs. 3 and 4 show the influence of λ parameter on the heat and concentration distributions respectively. Due to squeezing of the fluid the velocity increases and subsequently falls the temperature of the fluid because warm nanoparticles are escaping rapidly, which results in lower temperature and the concentration of the fluid automatically reduces. Fig. 5 demonstrates the impact of velocity field for various values of magnetic field parameter M. It depicts that an increase in the value of M, velocity profile decreases, because Lorentz forces work against the flow and those regions where its influences dominates, it reduces velocity. After a certain distance, it increases. Fig. 6 demonstrates the characteristics of magnetic parameter M on heat distribution, which is increasing for higher values and drops for the small values of M. Actually the Lorentz force, decreasing, which depend on the magnetic field M, so decreasing M leads to decrease the Lorentz force and consequently decreases $\theta(\eta)$. The impact of Pr on the $\theta(\eta)$ and $\phi(\eta)$ are presented in Figs. 7 and 8. Clearly, it is seen that temperature and concentration distributions vary inversely with Pr, that is temperature distribution drop with large numbers of Pr and rise for lesser values of Pr. Physically, the fluids having a small number of Pr has larger thermal diffusivity and this effect is opposite for higher Prandtl number. Due to this fact large Pr cause the thermal boundary layer to decreases. The effect is even more diverse for the small number of Pr since the thermal boundary layer thickness is relatively large. On the other hand, increasing behaviour of concentration distribution is shown in Fig. 8 for increasing Pr values. Fig. 9 represents the influence of thermophoretic parameter Nt on heat profile $\theta(\eta)$. It is investigated that $\theta(\eta)$ is increased by varying thermophoretic parameter Nt. According to Kinetic Molecular theory increasing the number of particles & increasing number of active particles both can cause to increase in the heat factor. Fig. 10 represents the change in the concentration profile $\phi(\eta)$ due to change in the parameter Nt. The profile $\phi(\eta)$ decreases in suction and injection cases. In injection case, the decrement in $\phi(\eta)$ is slow as compare to fluid suction case. Figs. 11 & 12 shows the effect of Nb on $\theta(\eta)$ and $\phi(\eta)$ fields. Heat profile $\theta(\eta)$ is increased by varying values of Nb as shown in Fig. 11. Due to Kinetic molecular theory, the heat of the fluid increases due to the increase of Brownian motion. So the given result is in good agreement with the real situation. Similarly, Fig. 12 highlights the impact of the varying Nb parameter with respect to the concentration profile $\phi(\eta)$ on the domain, $0 \le \eta \le 1$. An increasing impact of $\phi(\eta)$ observed for both suction and injection in Fig. 12. A fast increment observed in $\phi(\eta)$ for fluid suction as compared to fluid injection. Fig. 13 displays the influence of Le on the concentration profile $\phi(\eta)$ where it is decreased when the number Le increases. Actually, it is the ratio of thermal diffusivity to the mass diffusivity. So, when the thermal diffusivity decreases it automatically decreases Le and also decreases concentration field. Fig. 14 displays the impact of radiation parameter Rd on the heat field $\theta(\eta)$. It is clearly observed that heat profile

$\theta(\eta)$ decreases with increasing values of Rd. It is a common observation that radiating a fluid or some other thing can cause to reduce the temperature of that particular.

5.1 Discussion about tables

This segment of the article is about table discussions. Table 1 displays numerical values of HAM solutions at different approximation using various values of different parameters. It is clear from the Table 1 that homotopy analysis technique is a quickly convergent technique. Physical quantities, such as skin-friction coefficient, heat flux and mass flux for engineering interest are calculated through Tables (2-4). Table 2 displays the impact of inserting parameters M and λ on Skin friction C_f. It is seen that growing value of M, λ increases the skin friction. Table 3 examines the influences of embedding parameters Nb, Nt and Pr on heat flux Nu. It is seen that increasing values of Nb, Nt reduce the heat flux Nu, where Pr increase the heat flux when it increased. Table 4 inspects the influences of Nb and Nt on mass flux Sh. The increasing value of Nb increase the mass flux where Nt decreases the mass flux. The higher value of R d reducing the mass flux. Moreover, Temperature decreases with the temperature jump parameter and increases with the thermal radiation parameter inside thermal boundary-layer.

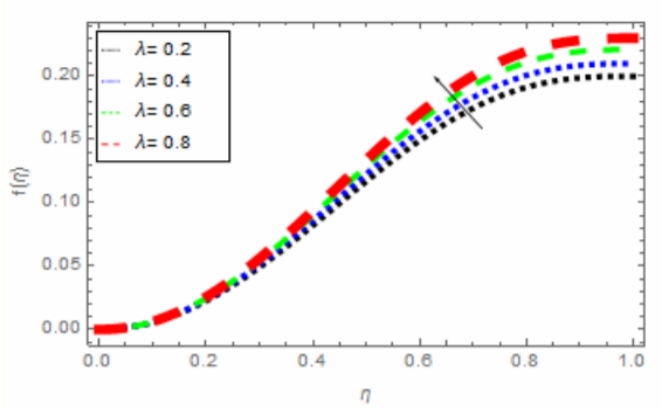

Fig. 2. Effect of λ on $f(\eta)$ when $\omega = 0.9$ and $M = 0.9$.

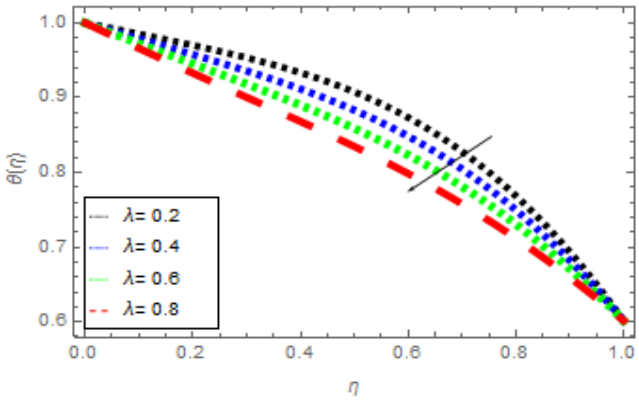

Fig. 3. Effect of λ on $\theta(\eta)$ when
$\omega = 0.9, Le = 0.4, Nb = 0.3, Nt = 0.1, \Pr = 0.6, Rd = 0.4.$

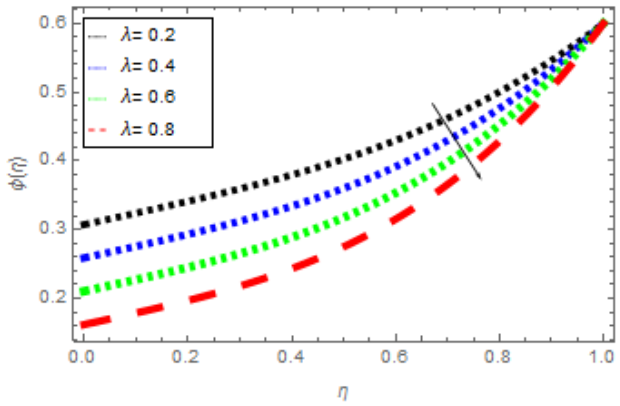

Fig. 4. Effect of λ on $\phi(\eta)$ when $\omega = 0.9, Le = 0.4, Nb = 0.3, Nt = 0.1, \Pr = 0.6, Rd = 0.4$.

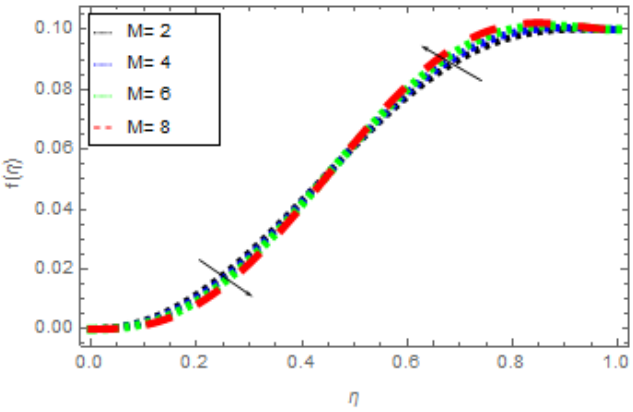

Fig. 5. Effect of M on $f(\eta)$ when $\omega = 0.1$ and $\lambda = 0.9$

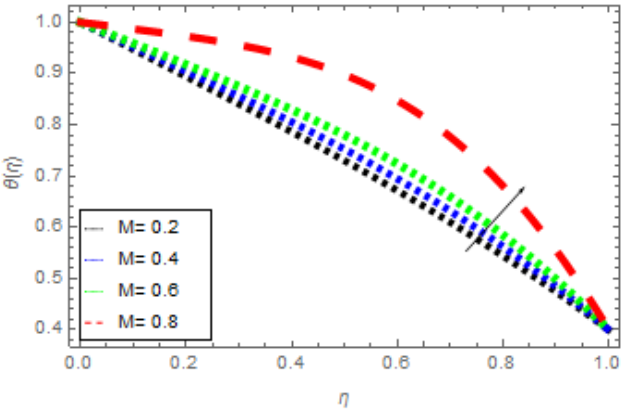

Fig. 6. Effect of M on $\theta(\eta)$ when $\omega = 0.9, Le = 0.3, \Pr = 0.5, Nt = 0.6, Nb = 0.1$ and $Rd = \lambda = 1$

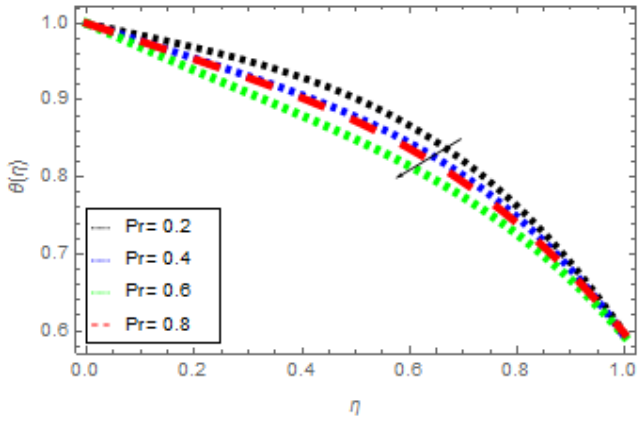

Fig. 7. Effect of $\Pr$ **on** $\theta(\eta)$ **when** $\omega = 0.9, Le = 0.3, Nb = 0.1, Nt = 0.6, \lambda = Rd = 0.4$

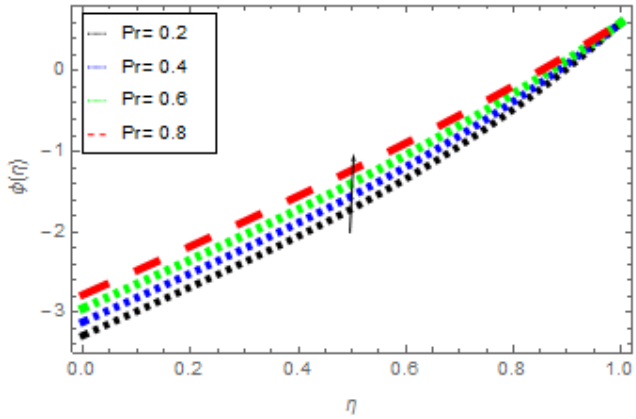

Fig. 8. Effect of $\Pr$ **on** $\phi(\eta)$ **when** $\omega = 0.9, Le = 0.3, Nb = 0.1, Nt = 0.6, \lambda = 0.4, \Pr = 0.2$

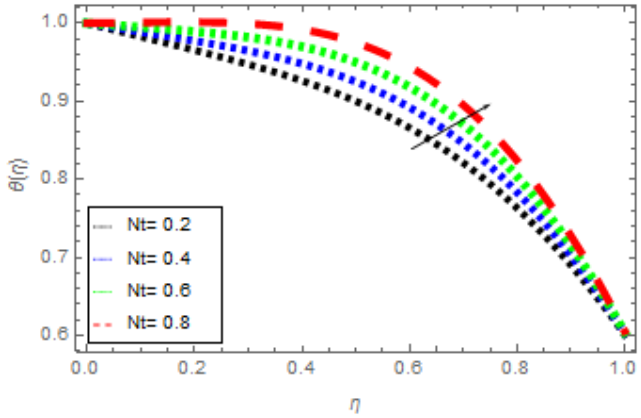

Fig. 9. Effect of Nt **on** $\theta(\eta)$ **when** $\omega = 0.9, Le = 0.3, Nb = 2, \lambda = Rd = 0.4, \Pr = 0.6$

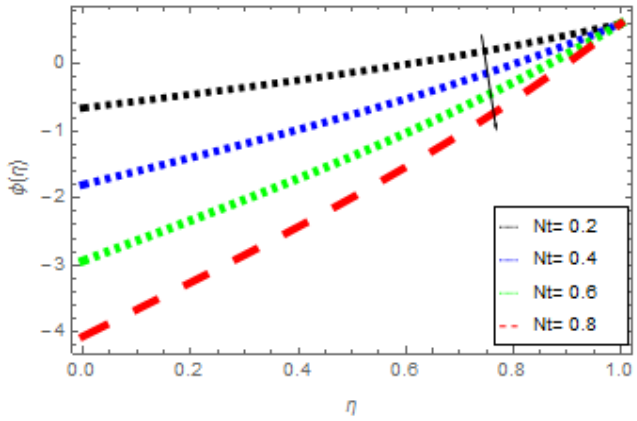

Fig. 10. Effect of Nt **on** $\phi(\eta)$ **when** $\omega = 0.8, Le = 0.3, Nb = 0.1, \lambda = 0.4, \Pr = 0.6$

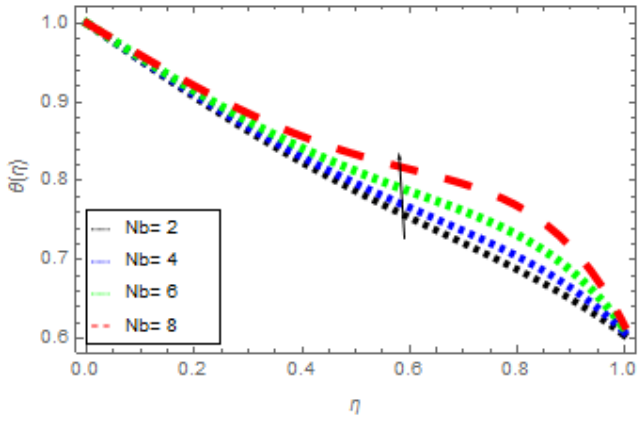

Fig. 11. Effect of Nb **on** $\theta(\eta)$ **when** $\omega = 0.8, Le = 0.3, Nt = 0.1, \lambda = Rd = 0.4, \Pr = 0.6$

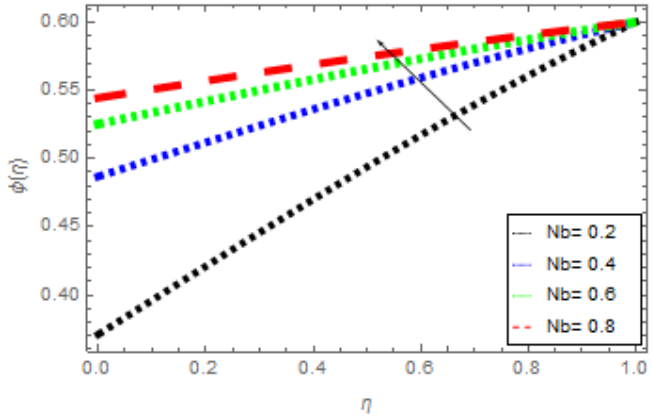

Fig. 12. Effect of Nb **on** $\phi(\eta)$ **when** $\omega = 0.8, Le = 0.3, Nt = 0.1, \lambda = 0.4, \Pr = 0.6$

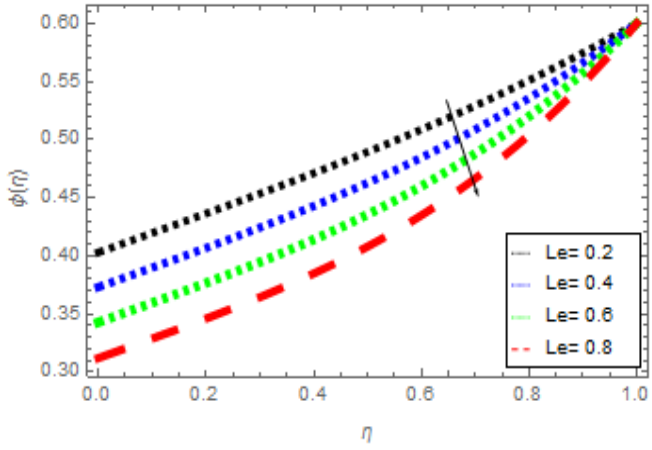

Fig. 13. Effect of Le **on** $\phi(\eta)$ **when** $\omega = 0.9, Le = 0.4, Nt = 0.1, Nb = 0.3, \lambda = 0.4, \Pr = 0.6$

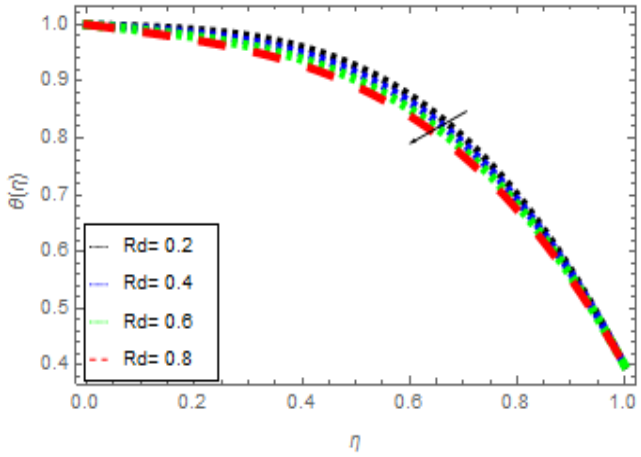

Fig. 14. Effect of Le **on** $\theta(\eta)$ **when** $\omega = Le = 1, \Pr = Nt = 0.6, Nb = 0.1, \lambda = 4$

Table 2. Displays the numerical values of the Skin Friction Co-efficient for various parameters where $Nt = Le = 0.6, Nb = 1,\ Sc = 0.8\ \ \&\ \ Pe = 0.7$.

M	λ	**Hayat et al. [43]**	$-\left(C_f \operatorname{Re}_x\right)^{\frac{1}{2}}$ **Present results**
0.1	1.5	2.279427	0.9957
0.5		2.287085	0.9999
1.0		2.309896	1.1051
1.5	1.5	2.175138	0.9957
	2.0	2.280654	1.2057
	2.5	2.385315	1.4947

Table 3. Displays the Numerical values of Local Nusselt number for unlike type parameters, where $\Pr = 0.7,\ \lambda = 0.5,\ Le = 0.6,\ Sr = Sc = 0.8,\ Pe = 0.7,\ \omega = 0.1,$ and $M = 0.5.$

Nb	*Nt*	Pr	**Alsaedi et al. [44]**	$-\theta'(0)$ **Present result**
0.5			0.8755	1.9501
1.0			0.8398	1.5546
1.5			0.8064	1.2013
2.0	0.5		0.8167	2.5923
	1.0		0.6971	1.7456
	1.5		0.5735	1.1196
	2.0	1.0	0.7472	1.0072
		1.5	0.8943	2.4609
		2.0	1.0270	2.1796

Table 4. Displays numerical type values of the Local-Sherwood number for different parameters Where, Sc=0.8, Le=0.6, Pr=Pe=0.7 and M=λ=0.5 .

Nb	*Nt*	**Alsaedi et al. [44]**	$-\phi'(0)$ **Present results**
0.2		0.5878	0.6624
0.6		0.9582	0.7910
1.0		1.0320	0.8518
0.2	0.5	0.5878	0.9901
	1.0	0.0858	0.9020
	1.5	-0.3914	0.8615

6 Concluding Remarks

In order to facilitate the readers the following conclusions are derived:

The observation of this investigation is regarding the effects of thermal radiations and magnetohydrodynamic (MHD) influences on squeezing nanofluid flowbetweentwo parallel plates. The key points are:

- When we increase thermal radiation parameter Rd , then it augments temperature of the boundary layer area in fluid layer. This increase leads to drop in the rate of cooling for nanofluid flow.
- Effects of squeezing parameter on temperature and concentration profiles are quite opposite to each other.
- It is observed that $\theta(\eta)$ is increased by varying thermophoretic parameter Nt .
- The larger values of Nb raises the kinetic energy of the nanoparticles, which result an increase in the heat profile.
- Effects of Brownian motion parameter on temperature and concentration profiles are quite the opposite from each other.
- The convergence of the homotopy method along with the variation of different physical parameters has been observed numerically.
- It is seen that increasing M and λ increase the skin friction C_f .
- It is seen that growing values of Nb and Nt reduce the heat flux Nu while large values of Pr increase the heat flux Nu .
- The increasing values of Nb increase the mass flux where Nt reduce the mass flux.

Acknowledgement

The authors are thankful to the anonymous reviewers and the Editor-in-Chief for the productive comments that led to positive enhancement in the paper.

Competing Interests

Authors have declared that no competing interests exist.

References

[1] Verma RL. A numerical solution to squeezing flow between parallel channels. Wear. 1981;72:89-95.

[2] Stefan MJ. Versuch Uber die scheinbare adhesion, Sitzungsberichte der Akademie der Wissenschaften in Wien.Mathematik-Naturwissen. 1874;69:713–721.

[3] Singh P, Radhakrishnan V, Narayan KA. Squeezing flow between parallel Plates Ingenieur- Archiv. 1990;60:274–281.

[4] Hayat T, Abbas T, Ayub M, Muhammad T, Alsaedi A. On squeezed flow of jeffrey Nanofluid between two parallel disks. Appl. Sci. 2016;6:346.

[5] Dib A, Haiahem A, Bou-Said B. Approximate analytical solution of squeezing unsteady nanofluid flow. Powder Tech. 2015;269:193–199.

[6] Masuda H, Ebata A, Teramae K, Hishinuma N. Alteration of thermal conductivity and viscosity of liquid by dispersing ultra-fine particles. Netsu Bussei. 1993;7(4):227-233.

[7] Choi SUS. Nanofluids from vision to reality through research. Journal of Heat Transfer. 2009;131: 1–9.

[8] Yu W, France DM, Robert JL, Choi SUS. Review and comparison of nanofluid thermal conductivity andheat transfer enhancement. Heat Transfer Engineering. 2008;29:432-46.

[9] Das SK, Choi SUS, Patel HE. Heat transfer in nanofluids-A review. Heat Transfer Engineering. 2006; 27:3-19.

[10] Muhammad S, Ali G, Shah Z, Islam S, Hussain SA. The rotating flow of magneto hydrodynamic carbon nanotubes over a stretching sheet with the impact of non-linear thermal radiation and heat generation/absorption. Appl. Sci. 2018;8.
DOI: 10.3390/app8040000

[11] Hamad MAA. Analytical solution of natural convection flow of a nanofluid over a linearly stretching sheet in the presence of magnetic field. International Communications in Heat and Mass Transfer. 2011;38:487–492.

[12] Hameed K, Muhammad H, Zahir S, Saeed I, Waris K, Muhammad S. The combined magneto hydrodynamic and electric field effect on an unsteady maxwell nanofluid flow over a stretching surface under the influence of variable heat and thermal radiation. Appl. Sci. 2018;8.
DOI: 10.3390/app8020160

[13] Sheikholeslami M, Ganji DD, Javed MY, Ellahi R. Effect of thermal radiation on magneto Hydrodynamics nanofluid flow and heat transfer by means of two phase model. J. Magn. Magn. Mater. 2015;374:36–43.

[14] Goodman S. Radiant-heat transfer between non gray parallel plates. Journal of Research of the National Bureau of Standards. 1957;58:Research Paper 2732.

[15] Borkakoti AK, Bharali A. Hydromagnetic flow and heat transfer between two horizontal plates, the lower plate being a stretching sheet. Q. Apple. Math. 1983;41:461–467.

[16] Attia HA, Kotb NA. Cairo, Egypt. MHD flow between parallel plates with heat transfer. Acta Mechanica. 1996;117:215-220.

[17] Sheikholeslami M, Ganji DD. Three dimensional heat and mass transfer in a rotating system using nanofluid. Powder Technol. 2014;253:789–796.

[18] Sheikholeslami M, Hatami M, Ganji DD. Nanofluid flow and heat transfer in a rotating system in the presence of a magnetic field. J. of Molecular Liquids. 2014;190:112-120.

[19] Sheikholeslami M, Rashidi MM, Alsaad DM, Firouzi F, Rokni HB, Domairry G. Steady nanofluid flow between parallel plates considering thermophoresis and Brownian effects. J. of King Saud University Science. 2016;28:380-389.

[20] Mahmoodi M, Kandelousi SH. Kerosene−alumina nanofluid flow and heat transfer for cooling application. J. Cent. South Univ. 2016;23:983-990.

[21] Mohyud-Din ST, Zaidi ZA, Khan U, Ahmed N. On heat and mass transfer analysis of the flow of ananofluid between rotating parallel plates. Aerospace Science and Technology. 2015;46:514-522.

[22] Rokni HB, Alsaad DM, Valipour P. Electro hydrodynamicnanofluid flow and heat transfer between twoplates. J. of Molecular Liquids. 2016;216:583–589.

[23] Azimi M, Riazi R. Heat transfer analysis of GO-water nano fluid flow between two parallel disk. Propulsionand Power Research. 2015;4:23–30.

[24] Hayat T, Qayyum A, Alsaadi F, Awais M, Abdullah M, Dobaie MA. Thermal radiation effects in squeezing flow of a Jeffery fluid. Eur. Phys. J. Plus. 2013;128:85.

[25] Ali F, Khan I, Haq SU, Shafie S. Influence of thermal radiation on unsteady free convection MHD flow of brinkman type fluid in a porous medium with Newtonian heating. Mathematical Problems in Engineering; 2013.
DOI.org/10.1155/2013/632394

[26] Khan SI, Khan U, Ahmed N, Mohyud-Din ST. Thermal radiation effects on squeezing flow casson fluid between parallel disks. Communications in Numerical Analysis. 2016;2016:92-107.

[27] Makinde OD, Animasaun IL. Thermophoresis and Brownian motion effects on MHD bioconvection of nanofluid with nonlinear thermal radiation and quartic chemical reaction past an Upper horizontal surface of a paraboloid of revolution. Journal of Molecular Liquids. 2016;733–743.
DOI: 10.1016/j.molliq.2016.06.047

[28] Avinash K, Sandeep N, Makinde OD, Animasaun IL. Aligned magnetic field effect on radiative bioconvection flow past a vertical plate with thermophoresis and Brownian motion. Defect and Diffusion Forum. 2017;377:127–140.
DOI: 10.4028/www.scientific.net/ddf.377.127

[29] Mahanthesh B, Gireesha BJ, Animasaun IL. Exploration of non-linear thermal radiation and suspended nanoparticles effects on mixed convection boundary layer flow of nanoliquids on a melting vertical surface. Journal of Nanofluids. 2018;7(5):833–843.
DOI: 10.1166/jon.2018.1521

[30] Nehad AS, Animasaun IL, Ibraheem RO, Babatunde HA, Sandeep N, Pop I. Scrutinization of the effects of Grash of number on the flow of different fluids driven by convection over various surfaces. Journal of Molecular Liquids. 2018;249:980-990.
DOI: 10.1016/j.molliq.2017.11.042

[31] Liao SJ. The proposed homotopy analysis method for the solution of nonlinear problems, PhD Thesis. Shangai Jiao Tong University; 1992.

[32] Liao SJ. An explicit totally analytic approximate solution for blasius viscous flow problems. Int. J. Nonlinear Mech. 1999;34:759–778.

[33] Liao SJ. On the analytic solution of magnetohydrodynamic flows of non-newtonian fluids over a stretching sheet. J. Fluid Mech. 2003;488:189–212.

[34] Liao SJ. On homotopy analysis method for nonlinear problems. Appl. Math. Comput. 2004;147:499–513.

[35] Liao SJ. An analytic solution of unsteady boundary layer flows caused by impulsively stretching plate. Commun. Nonlinear Sci. Numer. Simul. 2006;11:326–339.

[36] Liao SJ. An optimal homotopy-analysis approach for strongly nonlinear differential equations. Commun. Nonlinear Sci. Numer. Simul. 2010;15:2003–2016.

[37] Abbasbandy S. Homotopy analysis method for heat radiation equations. International Communications in Heat and Mass Transfer. 2007;34:380-387.

[38] Abbasbandy S, Shirzadi A. A new application of the homotopy analysis method: Solving the sturm-Liouville problems. Commun Nonlinear Sci Numer Simulat. 2010;16:112-126.

[39] Rashidi MM, Siddiqui AM, Asadi M. Application of homotopy analysis method to the unsteady squeezing flow of a second grade fluid between circular plates. Mathematical Problems in Engineering; 2010.
Doi.org/10.1155/2010/706840

[40] Rashidi MM, Mohimanian SA. Pour. Analytic approximate solutions for unsteady boundary-layer flow and heat transfer due to a stretching sheet by homotopy analysis. Nonlinear analysis: Modelling and Control. 2010;15:83–95.

[41] Hussain SA, Muhammad S, Ali G, Shah SIA, Ishaq M, Shah Z, Khan H, Tahir M, Naeem M. A bioconvection model for squeezing flow between parallel plates containing gyrotactic microorganisms with impact of thermal radiation and heat generation/absorption. Journal of Advances in Mathematics and Computer Science. 2018;27(4):1-22. Article no.JAMCS.41767.

[42] Bin-Mohsin B, Ahmed N, Adnan, Khan U, Mohyud-Din ST. A bioconvection model for a squeezing flow of nanofluid between parallel plates in the presence of gyrotactic microorganisms. Eur. Phys. J. Plus. 2017;132:187.

[43] Alsaedi A, Khan MI, Farooq M, Gull N, Hayat T. Magnetohydrodynamic (MHD) stratified bioconvective flow of nanofluid due to gyrotactic microorganisms. Advanced Powder Technology. 2017;28:288–298.

[44] Hayat T, Abbas T, Ayub M, Muhammad T, Alsaedi A. On squeezed flow of jeffrey nanofluid between two parallel disks. Appl. Sci. 2016;6:346.
DOI: 10.3390/app6110346

Peer-review history:
The peer review history for this paper can be accessed here (Please copy paste the total link in your browser address bar)
http://www.sciencedomain.org/review-history/25139